Journal of Magnetism and Magnetic Materials 322 (2010) 3576–3583

Contents lists available at ScienceDirect

Journal of Magnetism and Magnetic Materials

journal homepage: www.elsevier.com/locate/jmmm

Stationary thermal convection in a viscoelastic ferrofluid

D. Laroze [a,b,*], J. Martinez-Mardones [c], L.M. Pérez [d], R.G. Rojas [c]

[a] Max Planck Institute for Polymer Research, D 55021 Mainz, Germany
[b] Instituto de Alta Investigación, Universidad de Tarapacá, Casilla 7D, Arica, Chile
[c] Instituto de Física, Pontificia Universidad Católica de Valparaíso, Casilla 4059, Valparaíso, Chile
[d] Departamento de Ingeniería Metalúrgica, Universidad de Santiago de Chile, Av. Bernardo OHiggins 3363, Santiago, Chile

ARTICLE INFO

Article history:
Received 2 November 2009
Received in revised form
20 May 2010
Available online 15 July 2010

Keywords:
Thermal convection
Magnetic fluid
Viscoelastic fluid

ABSTRACT

We report theoretical and numerical results on convection for a magnetic fluid in a viscoelastic carrier liquid. We focus in the stationary convection for idealized boundary conditions. We obtain explicit expressions of convective thresholds in terms of the control parameters of the system. Close to bifurcation, the coefficients of the corresponding amplitude equation are determined analytically. Finally, the secondary instabilities are performed.

© 2010 Elsevier B.V. All rights reserved.

1. Introduction

Ferrofluids are magnetic fluids formed by a stable colloidal suspension of magnetic nanoparticles dispersed in a carrier liquid. Without an applied external magnetic field the orientations of the magnetic moments of the particles are random resulting in a vanishing macroscopic magnetization (magnetic disorder). An external magnetic field, however, easily orients the particles magnetic moments and a large (induced) magnetization is obtained. There are two main features that distinguish ferrofluids from ordinary fluids, the polarization force and the body couple. In the last decades much efforts have been dedicated to study the phenomenon of convective mechanism in ferrofluids. In addition, heat transfer through magnetic fluids, in particular, has been one of the leading area of scientific study due to its technological applications [1]. The ferrofluid convection has application in high-power capacity transformer system where the ferrofluid is used as a material in the core as well as a coolant in the transform. To activate convective cooling, knowledge of concentration gradient, which will induce convection, is required. An important application of ferrofluids lies in biomedicine where the carrier liquid is blood [2–6]; and it has a rheological properties [7–9]. In addition, when a magnetic field is applied, the ferrofluid can shown additional rheological properties such as magneto-viscosity, adhesion properties, non-Newtonian behavior, among others [10–19]. Hence, a detailed study of viscoelastic magnetic fluids is quite important and in order.

The first continuum description of magnetic fluids was given by Neuringer and Rosensweig [20]. Later, Finlayson [21] studied the convective instability of a magnetic fluid for a fluid layer heated from below in the presence of a uniform vertical magnetic field. He discussed the cases of both, shear free and rigid horizontal boundaries using the linear stability method. Gotoh and Yamada [22] carried out a similar study by assuming the fluid to be confined between two magnetic pole pieces. A weakly nonlinear analysis in a strong external field was considered by Blennerhassett et al. [23]. The convective instability for a rotating layer in a magnetic fluid has been studied by Gupta and Gupta [24] and by Venkatasubramanian and Kaloni [25]. An amplitude equation for the stationary convection with idealized boundary condition was derived in Ref. [26]. The Küppers–Lortz instability for the case of a rotating magnetic fluid was formulated by Auernhammer and Brand [27]. Ryskin and Pleiner [28], using nonequilibrium thermodynamics, have derived a complete set of equations to describe ferrofluids in an external magnetic field. This description is made in terms of a binary mixture, where the magnetophoretic effect, as well as magnetic stresses, has been taken into account in the static and dynamic parts of the ferrofluid equations. When the magnetophoretic effect can be neglected, we have analyzed the thermal convection for rotating ferrofluids. For idealized boundary condition for the typical conductive state in the stationary case an analytical expression was found for the Rayleigh number as function of control parameters [29]. Recently, the weakly nonlinear analysis for stationary convection in a rotating magnetic binary mixture was studied [30]. Other effects, such as the buoyancy-surface tension effects, nonuniform thermal

* Corresponding author at: Max Planck Institute for Polymer Research, D 55021 Mainz, Germany.
E-mail address: david.laroze@gmail.com (D. Laroze).

0304-8853/$ - see front matter © 2010 Elsevier B.V. All rights reserved.
doi:10.1016/j.jmmm.2010.07.010

gradients, magnetization constitutive equations, etc., have also been studied in Refs. [31–37].

On the other hand, viscoelastic properties of fluids can be described by a the constitutive equation, which relates the stress and strain rate tensors. Finding this relation, which should generalize the linear dependence characteristic of Newtonian fluids, is the main purpose of rheology. The simplest constitutive equation capable of describing realistically the viscoelastic properties is given by the so-called Oldroyd model [38]. In this model, the stress tensor is decomposed into both a polymeric contribution and a solvent contribution. Studies of convection in such fluids have been performed by various authors for different cases, either with free-free or rigid-rigid boundary conditions [39–47]. It has been found that, besides the usual stationary convection, oscillatory states can also be obtained at onset. Which type of convection—stationary or oscillatory appears—first is determined by the values of the rheological parameters. Experimental measurements of oscillatory convection in viscoelastic mixtures were reported by Kolonder [48] in a DNA suspension; and the theoretical studies of the convection thresholds for binary viscoelastic mixtures in different types of fluids, can be found in Refs. [49–55].

In this work, we study a magnetic fluid in a viscoelastic carrier liquid. We introduce the rheologic properties in a constitutive equation for the extra stress tensor. As a first step, we only focus our work on the stationary convection for idealized boundary conditions. In particular, the linear stability analysis of the conduction state is performed in the framework of Navier–Stokes equations and we obtain explicit expressions for the convective thresholds in terms of the control parameters. The weakly nonlinear analysis for stationary convection is performed and the coefficients of the amplitude equation are calculated explicitly and we find that a supercritical–subcritical transition can appear as a consequence of the rheological properties. Finally, the secondary instabilities are considered, the phase dynamics is developed, and the physical range of parameters is studied.

The paper is organized as follows: In Section 2, the basic hydrodynamic equations for viscoelastic magnetic fluid convection are presented. In Section 3, the linear stability analysis of the conduction state is performed. In Section 4, the weakly nonlinear analysis is developed and explicit expressions for the coefficients of the stationary amplitude equation are found and the nature of the bifurcation is discussed. In Section 5, the pattern formation is analyzed. Finally, conclusions are presented in Section 6.

2. Theoretical model

We consider a layer of incompressible magnetic fluid in a viscoelastic carrier liquid, of thickness d, parallel to the xy-plane, with very large horizontal extension in a gravitational field $\mathbf{g}$ and subject to a vertical temperature gradient. The magnetic fluid properties can be modeled as electrically nonconducting superparamagnets. The magnetic field $\mathbf{H}$ is assumed to be placed in a parallel to $\hat{\mathbf{z}}$. It would be homogeneous, if the magnetic fluid were absent. Let us choose the z-axis such that $\mathbf{g}=-g\hat{\mathbf{z}}$ and that the layer has its interfaces at $z=-d/2$ and $d/2$. A static temperature difference across the layer is imposed, $T(z=-d/2)=T_0+\Delta T$ and $T(z=d/2)=T_0$. The set-up of the problem is shown in Fig. 1. Under the Boussinesq approximation, the balance equations read

$$\nabla\cdot\mathbf{v}=0, \tag{1}$$

$$\rho_0 d_t\mathbf{v}=-\nabla p_{eff}+\nabla\cdot\overline{\tau}+\rho\mathbf{g}+\mathbf{M}\cdot\nabla\mathbf{H}, \tag{2}$$

$$\frac{c_{v,\mathbf{H}}}{T_0}d_tT+\chi_T\mathbf{H}_0\cdot d_t\mathbf{H}=\overline{\kappa}\nabla^2T+\vartheta\mathbf{H}_0\cdot\nabla^2\mathbf{H}, \tag{3}$$

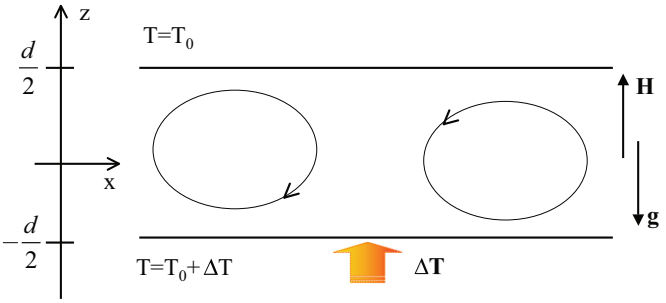


Fig. 1. A vertical cut through the fluid layer. Note the y-axis point into the xz-plane.

where $d_tf=\partial_tf+\mathbf{v}\cdot\nabla f$ is the convective derivative, $\mathbf{v}$ is the velocity field, p_{eff} is the effective pressure, ρ is the mass density, ρ_0 is a reference mass density, $\overline{\tau}$ is the extra stress tensor, $\mathbf{M}$ is the magnetization field, $c_{v,\mathbf{H}}$ is the specific heat capacity at constant volume and magnetic field, T is the temperature, T_0 is a reference temperature, χ_T is the pyromagnetic coefficient and $\overline{\kappa}$ is the thermal diffusivity.

For the total density we use the following linear state equation:

$$\rho=\rho_0(1-\alpha_T\Delta T+\alpha_H\mathbf{H}_0\cdot\Delta\mathbf{H}), \tag{4}$$

where α_T and α_H are the thermal and the magnetic expansion coefficients, respectively; and $\Delta f=f-f_0$. In addition, for the magnetic field $\mathbf{H}$ and the magnetic induction $\mathbf{B}$, we suppose that the system is not conductive, that is, it is governed by the Maxwell equations,

$$\nabla\cdot\mathbf{H}=\mathbf{0}, \tag{5}$$

$$\nabla\cdot\mathbf{B}=0. \tag{6}$$

We assume a linear the relationship between these fields $\mathbf{B}=\mathbf{H}+\mathbf{M}$ and note that from Eq. (5) the magnetic field can put in the form of a scalar magnetic potential $\mathbf{H}=-\nabla\phi$. For the magnetization field we use the typical phenomenological state equation $\mathbf{M}=\hat{\mathbf{H}}M(T,H)$ with

$$M(T,H)=M_0-\chi_T\Delta T+\chi_H\mathbf{H}_0\cdot\Delta\mathbf{H}. \tag{7}$$

A constitutive equation relating the extra stress tensor $\overline{\tau}$ and the shear rate has to be introduced. In a normal incompressible fluid, the extra stress tensor is related to the strain tensor via the Newton law, $\overline{\tau}=2\nu\overline{\boldsymbol{D}}$, where $\overline{\boldsymbol{D}}$ is the symmetric part of the velocity field gradient and ν is the viscosity. But, usually, a more general constitutive relation between stress and strain rate $\overline{\tau}=\overline{\tau}(\overline{\boldsymbol{D}})$ is necessary to describe the behavior of complex polymeric fluids. This relation is subjected to symmetry restrictions. A type of constitutive relation that satisfies these restrictions and that may be further justified by the kinetic theory of dumbbells has been proposed by Oldroyd [38]. These models, developed in the 1950s, include particular cases that are widely used for different kinds of polymeric solutions. In the Oldroyd model, the constitutive equation is written as

$$(1+\lambda_1D_t)\overline{\tau}=2\nu(1+\lambda_2D_t)\overline{\mathbf{D}}, \tag{8}$$

where ν is the static viscosity, λ_1 is the relaxation time, and λ_2 is the retardation time, parameters which characterize viscoelasticity. The symbol D_t in Eq. (9) denotes an invariant (frame-indifferent) time derivative, defined as

$$D_t\overline{\tau}=d_t\overline{\tau}+\overline{\tau}\cdot\overline{\mathbf{W}}-\overline{\mathbf{W}}\cdot\overline{\tau}+a(\overline{\tau}\cdot\overline{\mathbf{D}}+\overline{\mathbf{D}}\cdot\overline{\tau}), \tag{9}$$

where $\overline{\mathbf{W}}$ is the skew-symmetric part of the velocity field gradient; also a is a phenomenological parameter in the range -1 to $+1$. For $a=-1$ the lower convectec Jeffreyś model

(Oldroyd B) is obtained, $a=0$ leads to the so-called corotational Jeffreyś model, and $a=1$ to the upper convected Jeffreyś model (Oldroyd A). Let us comment that the coefficient a is not completely free in choosing [56]; $\lambda_2=0$ gives a Maxwellian fluid, while a Newtonian fluid requires $\lambda_1=0$ and $\lambda_2=0$.

Now we analyze the boundary conditions (BCs); a static temperature difference across the layer is imposed, $T(z=-d/2)=T_0+\Delta T$ and $T(z=d/2)=T_0$; as the magnetic BCs we use the typical continuity conditions $\mathbf{n}\times(\mathbf{H}_{in}-\mathbf{H}_{ex})=\mathbf{0}$ and $\mathbf{n}\cdot(\mathbf{B}_{in}-\mathbf{B}_{ex})=0$, where $\mathbf{n}$ is a unit vector normal to the boundaries. Moreover, for the velocity field we will consider (unrealistic) free interfaces. Hence, from Eqs. (1)–(8) and using these boundary conditions the conductive basic state is

$$\mathbf{v}_{con}=\mathbf{0}, \tag{10}$$

$$T_{con}(z)=\overline{T}-\beta z, \tag{11}$$

$$\mathbf{H}_{con}(z)=\mathbf{H}_0(1+\lambda\beta z), \tag{12}$$

where $\beta=(\Delta T/d)$ and $\lambda=\chi_T/(1+\chi_H)$. Therefore the perturbation equation of the conducting state can be written as

$$\nabla\cdot\mathbf{v}=\mathbf{0}, \tag{13}$$

$$(\partial_t+\mathbf{v}\cdot\nabla)(\theta-M_4\partial_z\phi)=(1-M_4)w+\nabla^2\theta, \tag{14}$$

$$P^{-1}(\partial_t+\mathbf{v}\cdot\nabla)\mathbf{v}=-\nabla p_{eff}+\nabla\cdot\overline{\boldsymbol{\tau}}+R_a\Pi_1\hat{\mathbf{z}}+RaM_1\theta\nabla(\partial_z\phi), \tag{15}$$

$$(1+\Gamma D_t)\overline{\boldsymbol{\tau}}=(1+\Gamma\Lambda D_t)\overline{\boldsymbol{D}}, \tag{16}$$

$$(\partial_{zz}+M_3\nabla_\perp^2)\phi-\partial_z\theta=0, \tag{17}$$

$$\nabla^2\phi_{ext}=0, \tag{18}$$

where $\Pi_1(\theta,\phi)=(1+M_1)\theta-(M_1-M_5)\partial_z\phi$. Also, the following groups of dimensionless numbers have been introduced: (a) (pure fluids) The Rayleigh number, $Ra=\alpha_T g\Delta T d^3/\kappa\nu$, accounting for buoyancy effects; and the Prandtl number, $P=\nu/\kappa$, relating viscous and thermal effects. (b) (magnetic fluid) The strength of the magnetic force relative to buoyancy, $M_1=\beta\chi_T^2H_0^2/(\rho_0 g\alpha_T(1+\chi))$; the nonlinearity of the magnetization, $M_3=1-(\chi_H H_0^2)/(1+\chi)$, a measure of the deviation of the magnetization curve from the linear behavior $M_0=\chi_H H_0$; the relative strength of the temperature dependence of the magnetic susceptibility $M_4=\chi_T^2H_0^2T_0/c_{v,\mathbf{H}}(1+\chi)$; and the ratio of magnetic to thermal buoyancy $M_5=\alpha_H\chi_T H_0^2/(\alpha_T(1+\chi))$. (c) (viscoelastic fluid) The Deborah number, $\Gamma=\lambda_1\overline{\kappa}/d^2$, and the ratio between retardation and stress relaxation times, $\Lambda=\lambda_2/\lambda_1$. For $\Gamma=0$ one recovers a Newtonian fluid while for $\Lambda=0$ a Maxwellian fluid is obtained.

Let us comment on the numerical values of the parameters; the parameter Ra can be changed by several orders of magnitude, while a typical value for P in viscoelastic fluid is $P\sim10^0-10^3$. The magnetic numbers have the following order of magnitude $M_1\sim10^{-4}-10^1$, $M_3\sim10^0$, $M_4\sim M_5\sim10^{-6}$ [28,29]. For aqueous suspensions it is suggested that the Deborah number is about $\Gamma\sim10^{-3}-10^{-1}$ [48,57–59], but for other kinds of viscoelastic fluids the Deborah number can be of the order of $\Gamma\sim10^3$. Unfortunately, no experimental data are available for either the retardation or the stress relaxation times, so we treat Λ as arbitrary in the range (0, 1). The values of M_4, M_5 are very small, so in the following analysis we are not going to take them into account.

For the sake of simplicity, the analysis is limited to a two-dimensional motion. Therefore, we can use a stream function $\psi(x,z,t)$ that gives the velocity field (v_x,v_z). Due to its symmetry properties, the extra stress tensor has only three independent coefficients: $\tau_{xx},\tau_{zz},\tau_{zx}=\tau_{xz}$. Instead of these individual components, the following three scalar quantities are usually considered in rheology, the trace $U=\tau_{xx}+\tau_{zz}$, the normal stress difference $S=\tau_{xx}-\tau_{zz}$, and the in-plane shear stress τ_{zz}. Using the afore mentioned assumptions, we can write Eqs. (13)–(17) in the following way:

$$\pounds\mathbf{u}+\mathbf{N}(\mathbf{u}|\mathbf{u})=0, \tag{19}$$

with $\mathbf{u}=(\psi,\theta,\phi,\tau,S,U)^T$ and where $\pounds$ is the spatio-temporal linear operator and $\mathbf{N}$ stands for the nonlinear part of the respective equations. Both they are given explicitly in the Appendix. In the next sections we will develop the linear and weakly nonlinear analysis for stationary convection.

3. Linear stability analysis

In order to calculate the linear stability analysis, we only need the linear parts of Eq. (19). The space-time dependencies of $\mathbf{u}(\mathbf{r},t)$ are separated using a normal mode expansion,

$$\mathbf{u}(\mathbf{r},t)=\tilde{\mathbf{u}}(z)\exp[i\,kx+st], \tag{20}$$

with $\tilde{\mathbf{u}}=(\tilde{\psi},\tilde{\theta},\tilde{\phi},\tilde{\tau},\tilde{S},\tilde{U})^T$, where k is the horizontal wave-number and where $s=\sigma+i\Omega$ denotes the complex eigenvalues; σ is the growth factor of a perturbation, and Ω its frequency.

With the purpose to find analytical expressions we impose the following boundary conditions $\tilde{\psi}=D^2\tilde{\psi}=\tilde{\theta}=D\tilde{\phi}=\tilde{\tau}=D\tilde{S}=\tilde{U}=0$ in $z=\pm1/2$; with $D^nf=\partial_z^nf$. In what follows we will only focus on the stationary convection case. Hence, the eigenvalue problem gives the Rayleigh number and the stationary bifurcation is obtained by the condition of marginal linear stability $s=0$. For the fundamental mode, we can introduce the ansatz for the stream function,

$$\tilde{\psi}(z)=\cos(\pi z). \tag{21}$$

Therefore, $\pounds\mathbf{u}=0$ leads

$$\tilde{\theta}(z)=-\frac{k}{q^2}\cos(\pi z), \tag{22}$$

$$\tilde{\phi}(z)=\frac{\pi}{q^2\varrho}\sin(\pi z), \tag{23}$$

$$\tilde{\tau}(z)=-\Sigma\cos(\pi z), \tag{24}$$

$$\tilde{S}(z)=4\pi k\sin(\pi z), \tag{25}$$

$$\tilde{U}(z)=0, \tag{26}$$

where $q^2=k^2+\pi^2$, $\Sigma=\pi^2-q^2$ and $\varrho=M_3k^2+\pi^2$.

As solvability condition for the linear part of Eq. (19) we find the following relation between the parameters as the condition to have a stationary instability (marginal curve),

$$Ra_s=\frac{\varrho q^6}{k^2(k^2M_1M_3+\varrho)}. \tag{27}$$

Eq. (27) is the same as for simple ferrofluids [21]; hence the viscoelastic effects do not show up here. The minimum of the marginal curve ($\partial_k Ra_s=0$) gives the critical wave-number k_c and, the critical Rayleigh number, Ra_{sc}, is obtained by replacing k by k_c in Eq. (27). Fig. 2 shows the critical Rayleigh number, Ra_{sc}, as a function of the strength of the magnetic force relative to the buoyancy force, M_1. We observe that it decreases as M_1 increases, therefore the magnetic effects are destabilizing.

Finally let us remark that in viscoelastic fluids a range of parameters exists where an oscillatory instability can appear. Here we give only a short introduction on this type of bifurcation, while the complete analysis will be published in forthcoming works. This instability occurs when $s=i\Omega$ with $\Omega\epsilon\Re$. In general, an oscillatory bifurcation produces a complex eigenvalue, which

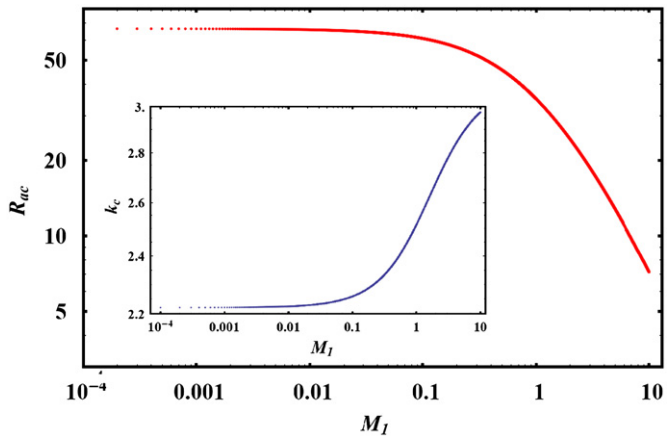


Fig. 2. Critical Rayleigh number, Ra_{sc}, as a function of M_1 at $M_3=1.1$. The inset shows the critical wave-number, k_c, as a function of M_1 at $M_3=1.1$.

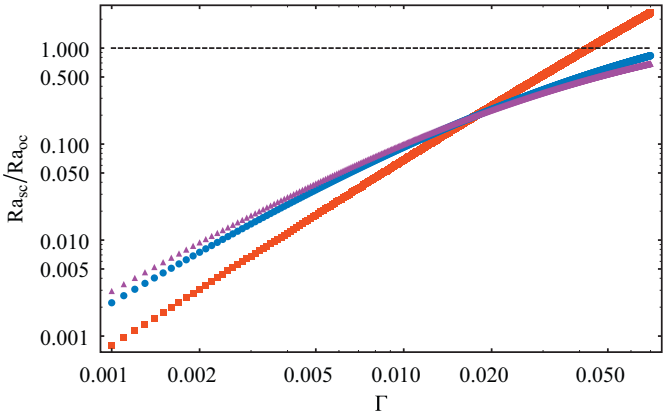


Fig. 3. Ra_{sc}/Ra_{oc}, as a function of Γ at $M_1=1$, $M_3=1.1$ and $P=10$ for different values of Λ, where {■,●,▲} depict $\Lambda=\{0,0.3,0.5\}$.

in our case is the Rayleigh number. However, since Ra is a physical quantity, its complex part must vanish and the real part gives the marginal stability curve $Ra_o(k,\Omega)$. Actually, one has to select a specific Ω in order to get a vanishing imaginary part of Ra_o. This condition, together with the critical condition $\partial_k \Re[Ra_o]=0$, determines the critical wave number k_{oc}. Replacing k by k_{oc} one obtains the critical value Ra_{oc} and the corresponding critical frequency, Ω_c. For idealized boundary conditions and for $s\neq 0$, the general expression for the Rayleigh number can be cast in the form

$$Ra=\frac{q^2\varrho(q^2+s)(s+\Gamma s^2+Pq^2(1+s\Lambda\Gamma))}{k^2(k^2M_1M_3+\varrho)P(1+s\Gamma)}. \tag{28}$$

Using (27), one can write it in the following way:

$$\frac{Ra}{Ra_s}=\frac{(q^2+s)(s+\Gamma s^2+Pq^2(1+s\Lambda\Gamma))}{q^4P(1+s\Gamma)}. \tag{29}$$

This factorization shows explicitly the dependence of the rheology in Ra. Using (28) and the criterion discussed before, one can calculate Ra_{oc}. Since our analysis is focused on the stationary regime, we are here investigating the range of parameters where the stationary bifurcation is the first one. Fig. 3 shows the ratio between stationary and the oscillatory Rayleigh numbers as a function of the Deborah number, for different values of the ratio between retardation and stress relaxation times, Λ. One can observe that $Ra_{sc}/Ra_{oc}<1$ for small values of Γ and its range increases when Λ increases. This implies that in the range of $\Gamma\sim 10^{-4}-10^{-2}$ the stationary bifurcation is the first one; while for large value of Γ the oscillatory bifurcation can be the first one.

4. Weakly nonlinear analysis

In this section, the evolution of the pattern is developed by means of a multiple scale analysis used by Newell and Whitehead [60] and Segel [61]. We will assume that a small amplitude convection cell is imposed on the basic flow. For values of the control parameter Ra_s given by Eq. (27) close to its threshold value Ra_{sc}, the bifurcation parameter will be

$$\epsilon^2=\frac{Ra_s-Ra_{sc}}{Ra_{sc}}. \tag{30}$$

We expand all function in ϵ and assume that all variations of the linearized solutions can be incorporated into an amplitude function A. If this amplitude is of size of ϵ ($O(\epsilon)$) then the interaction of the cell with itself forces a second harmonic and a mean state of correction of size $O(\epsilon^2)$ and these in turn drive an $O(\epsilon^3)$ correction to the fundamental component of the imposed roll. A solvability criterion for this last correction yields an equation for the complex amplitude $A(X,T)$ of the imposed disturbance, the Ginzburg Landau (GL) equation. The z-dependence is contained entirely in the sine and cosine functions, which ensures that the free-free boundary conditions are satisfied. Therefore, our expansion is

$$\mathbf{u}\longrightarrow \epsilon A\{\mathbf{u}^{(0)}+\epsilon\mathbf{u}^{(1)}+\epsilon^2\mathbf{u}^{(2)}+\Theta(\epsilon^3)\}. \tag{31}$$

Here $\mathbf{u}^{(0)}$ is the linear solution. Inserting the above equation into the governing equation (19), and expanding them, we obtain a hierarchy of equations

$$\epsilon^1: \quad \pounds^{(0)}\mathbf{u}^{(0)}=0, \tag{32}$$

$$\epsilon^2: \quad \pounds^{(0)}\mathbf{u}^{(1)}=-N(\mathbf{u}^{(0)}|\mathbf{u}^{(0)}), \tag{33}$$

$$\epsilon^3: \quad \pounds^{(0)}\mathbf{u}^{(2)}=-\pounds^{(2)}\mathbf{u}^{(0)}-N(\mathbf{u}^{(0)}|\mathbf{u}^{(1)})-N(\mathbf{u}^{(1)}|\mathbf{u}^{(0)}). \tag{34}$$

These equations must be solved iteratively thereby fulfilling the solvability condition,

$$\langle \mathbf{u}^{\dagger}|r.h.s.\rangle=\mathbf{0}, \tag{35}$$

where $\mathbf{u}^{\dagger}$ are the solution of the kernel of the linear adjoint problem ($\pounds^{+}\mathbf{u}^{\dagger}=0$). Here, $r.h.s$ means the corresponding right hand side of the perturbation equations and $<|>$ denotes the inner product which is an average over a suitable volume. The solvability condition at $O(\epsilon^3)$ leads to an equation for the amplitude A of the type [62]

$$\tau_0\frac{\partial A}{\partial t}=\xi_0^2\frac{\partial^2}{\partial x^2}A+\epsilon^2A-g|A|^2A. \tag{36}$$

Eq. (36) is the GL equation and describes the variation of the slow time scale $\epsilon^2 t$ and slow spatial scale ϵx, perpendicular to the rolls. For $\epsilon=0$, we do not get a GL equation. The coefficients of this equation can be calculated as [27]

$$\tau_0=\left(Ra_s\frac{\partial\sigma}{\partial Ra_s}\right)^{-1}_{Ra_{sc}}, \tag{37}$$

$$\xi_0^2=\frac{1}{2Ra_{sc}}\left(\frac{\partial^2 Ra_s}{\partial k^2}\right)_{Ra_{sc}}, \tag{38}$$

$$g=\tau_0\langle\mathbf{u}^{\dagger}|N(\mathbf{u}^{(0)}|\mathbf{u}^{(1)})t\rangle_{Ra_{sc}}+\tau_0\langle\mathbf{u}^{\dagger}|N(\mathbf{u}^{(1)}|\mathbf{u}^{(0)})\rangle_{Ra_{sc}}. \tag{39}$$

The coefficients τ_0 and ξ_0^2 are known as growth rate amplitude and the curvature of the marginal stability curve, respectively. The coefficient g is known as nonlinear cubic coefficient and for $g>0$ we get forward bifurcation (supercritical bifurcation), for $g<0$ we get backward bifurcation (subcritical bifurcation), and at $g=0$ we get tricritical bifurcation point which is the

transition point between subcritical and supercritical bifurcation; and this critical transition also is denoted supercritical quintic bifurcation. After straight-forward calculations, the explicit expressions of these coefficients can be written as

$$\tau_0 = \frac{1+P^{-1}}{q_c^2} - \Xi, \tag{40}$$

$$\xi_0^2 = \frac{2}{q_c^2} - \frac{M_1 M_3 \pi^2}{\varrho_c((1+M_1)M_3 k_c^2 + \pi^2)}, \tag{41}$$

$$\begin{aligned} g = {} & \frac{\pi^2 q_c^2 (M_3(1+2M_1)k_c^2 + \pi^2)}{2(k_c^2(1+M_1)M_3 + \pi^2)} \\ & + \frac{a^2 \Xi \Gamma}{q_c^4}(9q_c^{16} + 8\pi^2 k_c^2 \Sigma_c^4 + 144\pi^4 k_c^4) \\ & - \frac{\Xi\Gamma}{q_c^4}(9q_c^8 \Sigma_c^4 + 4\pi^2 k_c^2 q_c^8 + 64\pi^4 k_c^4), \end{aligned} \tag{42}$$

where $\Xi = \Gamma(1-\Lambda)$. Note that, we can recover some previous results, for instance, if we put $\Lambda \equiv 1$ we obtain

$$\tau_{0,\mathcal{N}} = \frac{1+P^{-1}}{q_c^2}, \tag{43}$$

$$\xi_{0,\mathcal{N}}^2 = \frac{2}{q_c^2} - \frac{M_1 M_3 \pi^2}{\varrho_c((1+M_1)M_3 k_c^2 + \pi^2)}, \tag{44}$$

$$g_{\mathcal{N}} = \frac{\pi^2 q_c^2 (M_3(1+2M_1)k_c^2 + \pi^2)}{2(k_c^2(1+M_1)M_3 + \pi^2)}. \tag{45}$$

The last equations show exactly the coefficients for a magnetic Newtonian fluid found in Ref. [26]. In addition, imposing $M_1 = M_3 \equiv 0$, the Eqs. (40)–(42) are reduced to

$$\tau_{0,\mathcal{V}} = \frac{2(1+P^{-1})}{3\pi^2} - \Xi, \tag{46}$$

$$\xi_{0,\mathcal{V}}^2 = \frac{4}{3\pi^2}, \tag{47}$$

$$\begin{aligned} g_{\mathcal{V}} = {} & \frac{3\pi^4}{4} + \frac{a^2 \Xi \Gamma \pi^2}{576}(18\,432 + 64\pi^5 + 59\,049\pi^{10}) \\ & - \frac{\Xi\Gamma\pi^2}{576}(8192 + 2592\pi^6 + 729\pi^{10}). \end{aligned} \tag{48}$$

These expressions are exactly the coefficients for a viscoelastic fluid found in Ref. [50].

Also, we remark that ξ_0^2 does not depend on the viscoelastic properties. Figs. 4 and 5 show the linear coefficients τ_0^{-1} and ξ_0^2 as a function of M_1 at $M_3 = 1.1$, respectively. From Fig. 4 we observe that τ_0 decreases when M_1 and it increases when Λ increases. From Fig. 5 we observe that ξ_0^2 decreases when M_1 increases.

Figs. 6 and 7 show the behavior of the nonlinear cubic coefficient, g. Fig. 6 shows the ratio between g and the Newtonian cubic nonlinear coefficient, $\delta g = g/g_N$, as a function of M_1 for different values of the Deborah number Γ. We observe that δg increases when M_1 increases and that δg decreases when Γ decreases. Actually, δg has a power law dependence on M_1, so it can be expressed as $\delta g = \overline{\delta g}/2 + \sum_{j=1}^{N} a_j M_1^{b_j}$. We fit these curves with $N = 5$ and get a very good agreement, for example, for $\Gamma = 0.1$ the corresponding values of $\{\overline{\delta g}, a_j, b_j\}$ are: $\overline{\delta g} = 1515.35$, $a_1 = -5.41684$, $a_2 = 0.395149$, $a_3 = 214.71$, $a_4 = 2.15654$, $a_5 = -0.103244$, $b_1 = 3.26713$, $b_2 = 1.73023$, $b_3 = 0.258623$, $b_4 = 0.938658$ and $b_5 = 0.917454$. The inset of Fig. 6 shows the comparison between this fit and δg. Fig. 7 shows δg as a function of M_3 for different values of M_1 and we note that δg increases until a maximum value and after that it decreases. Notice that, the maximum value of δg increases when M_1 increases as shown by the inset.

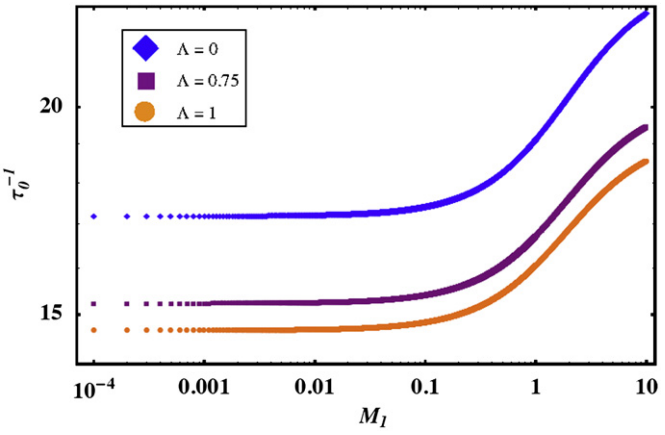


Fig. 4. τ_0^{-1} as a function of M_1 at $\Gamma = 0.01$, $M_3 = 1.1$ and $P = 100$ for $\Lambda = 0$, 0.75 and 1.

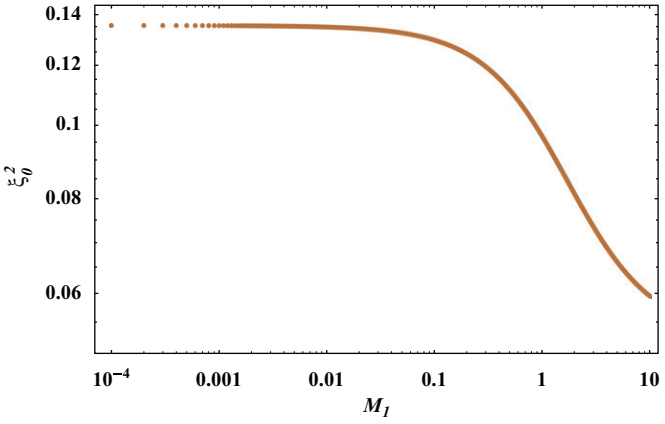


Fig. 5. ξ_0^2 as a function of M_1 at $M_3 = 1.1$.

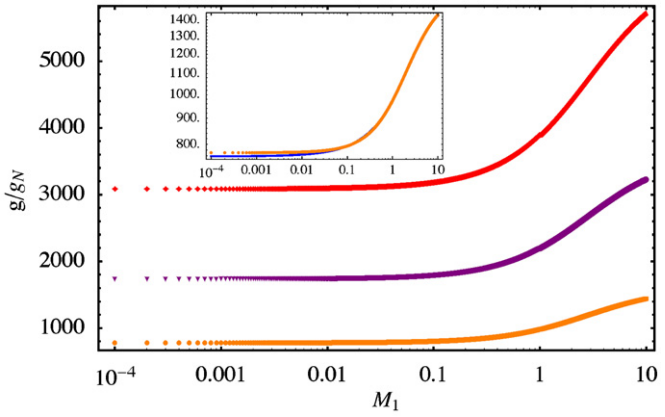


Fig. 6. g/g_N as a function of M_1 at $\Lambda = 0.75$, $M_3 = 1.1$, $a = 1$ whit different values of Γ where {•,▼,◆} depict $\Gamma = \{0.1, 0.15, 0.2\}$, respectively. The inset shows a fit for $\Gamma = 0.1$.

Form Eq. (42) we find that for $g = 0$ the following relation is satisfied:

$$\Gamma_T^2 = \frac{\pi^2 (k_c^2(1+2M_1)M_3 + \pi^2) q_c^6}{\ell_c(\eta_c - 64k_c^2\pi^4 - 4k_c^2\pi^2 q_c^8 - 9q_c^8 \Sigma_c^4)}, \tag{49}$$

where $\ell = 2(\pi^2 + (1+M_1)M_3 k^2)(\Lambda - 1)$ and $\eta = a^2(144k^2\pi^4 + 9q^{16} + 8k^2\pi\Sigma^4)$. Hence, a supercritical–subcritical transition appears. Since $\Gamma \geq 0$ and $0 \leq \Lambda \leq 1$, Eq. (49) has the following restrictions: $\eta_c - 64k_c^2\pi^4 - 4k_c^2\pi^2 q_c^8 - 9q_c^8 \Sigma_c^4 < 0$ and $\Lambda \neq 1$. These restrictions imply that the transition occurs for models likes corotational Jeffreyś model because a is near to zero. Also, note that this phenomenon occurs also

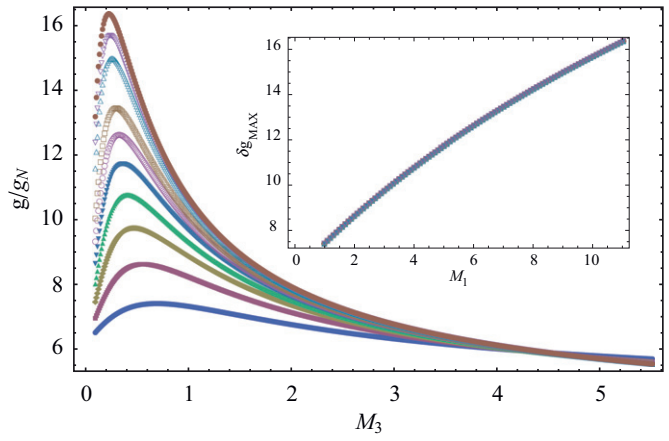


Fig. 7. g/g_N as a function of M_3 at $\Lambda=0$, $\Gamma=0.002$, $a=1$ with different values of M_1. The inset shows maximum value of g/g_N as a function of M_1.

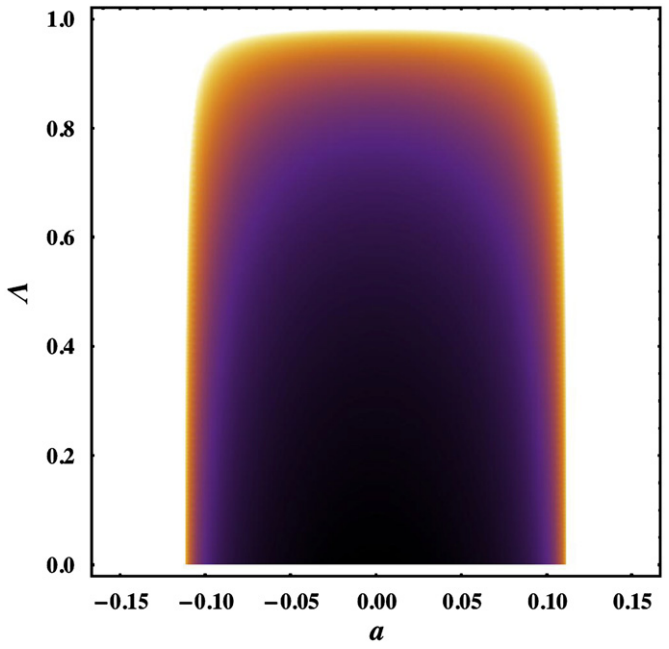


Fig. 8. $\Lambda-a$ phase diagram for the supercritical–subcritical transition in viscoelastic fluid.

for nonmagnetic viscoelastic fluid,

$$\Gamma_{T,\mathcal{V}}=\frac{12\sqrt{3}\pi}{\sqrt{(a^2n-m)(\Lambda-1)}}, \tag{50}$$

where $n=(18\,432+64\pi^5+59\,049\pi^{10})$ and $m=8192+81\pi^6(32+9\pi^4)$. Therefore, this transition is a consequence of the viscoelastic properties [55], as shown in Fig. 8. We remark that our analysis is valid for $g\geq 0$, and there is other range of physical parameters for $g<0$ and in this case it is necessary to use the Cubic-Quintic GL equation.

5. Pattern formation

In this section we develop the corresponding pattern formation based on the real GL equation. Note that the uniform solutions of Eq. (36) are $A_H=\{0,\pm\sqrt{\epsilon^2/g}\}$. The stationary case of the GL equation obtained by dropping the time derivative in Eq. (36), can be written as

$$\xi_0^2\frac{\partial^2 A}{\partial x^2}+\epsilon^2 A-g|A|^2A=0, \tag{51}$$

and an analytical solution is

$$A(x)=A_0\tanh(\zeta x), \tag{52}$$

where $A_0=\sqrt{\epsilon^2/g}$ and $\zeta=\sqrt{\epsilon^2/2\xi_0^2}$. Hence, the maximum of the steady amplitude A, denoted by $|A_{max}|$, is given by $|A_{max}|=\sqrt{\epsilon^2/g}$. We can use A_{max} to calculate the Nusselt number, Nu. This number measures the ratio of the total heat transfer across a horizontal plane to the heat transfer by conduction alone, and it can be expressed as $Nu=1+(\pi q_c)^2|A_{max}|^2/\sqrt{1+\epsilon^2}$; and from it, we get convection for $Nu>1$ and conduction for $Nu=1$.

Furthermore, increasing the Rayleigh number, the system will develop roll patterns corresponding to the steady solutions of the amplitude Eq. (36). These solutions form the family

$$A(x)=\sqrt{\frac{\epsilon^2-(p\xi_0)^2}{g}}\exp(px+\varphi), \tag{53}$$

where φ is an arbitrary phase. These solutions exist in the range $-\epsilon/\xi_0<p<\epsilon/\xi_0$, but their stability range is reduced, as usual, by the Eckhaus instability, and is thus given by $-\sqrt{3}\epsilon/(3\xi_0)<p<\sqrt{3}\epsilon/(3\xi_0)$.

Fig. 9 shows the stationary solutions (36) and (52). Both solutions are typical solutions of this equation; however, this model can exhibit a more complicated behavior, specially with different types of boundary conditions [63–65].

Now, let us analyze the phase dynamics. For this purpose we write Eq. (36) in the polar form $A=R\exp(i\Theta)$, hence the equation for R and for Θ are

$$\tau_0\partial_t R=\epsilon^2R-gR^3+\xi_0^2(\partial_{xx}R-R(\partial_x\Theta)^2), \tag{54}$$

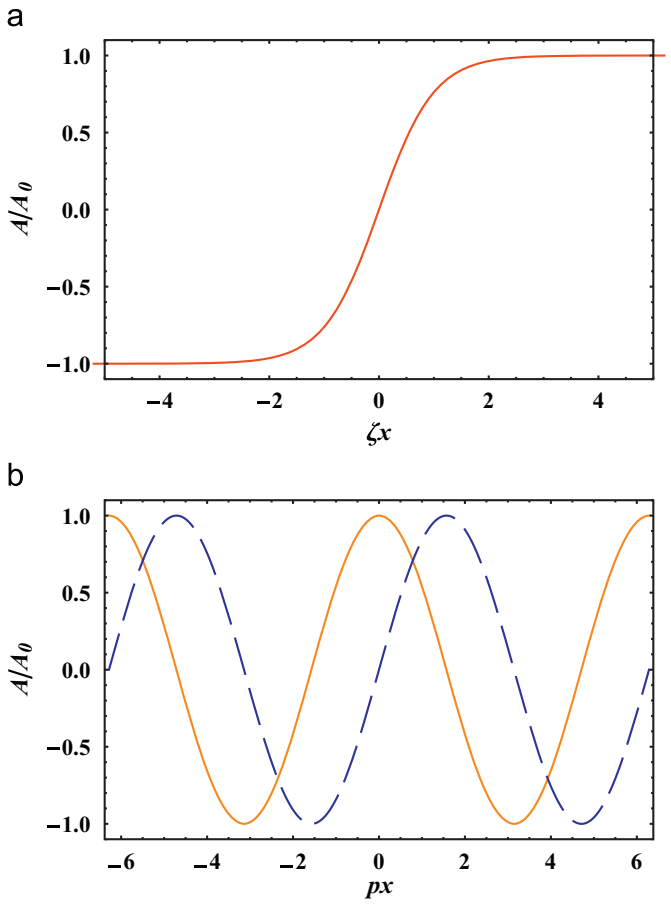


Fig. 9. Stationary solutions of the amplitude equation: (a) correspond to solution Eq. (52) and (b) correspond to Eq. (53) where the solid and dashed lines represent the real and imaginary part, respectively.

$$\tau_0 R\partial_t \Theta = \xi_0^2 (R\partial_{xx}\Theta + 2(\partial_x R)(\partial_x \Theta)). \tag{55}$$

The stationary solutions of these equations are $\Theta_0 = xp$ and $R_0 = \sqrt{(\epsilon^2 - (\xi_0 p)^2)/g}$. The perturbation for Θ is $\Theta(x,t) = \Theta_0(x) + \Phi(x,t)$ and we will assume that $\partial_t R \approx 0$ and that $R = R(\Theta)$, such that $R = R_0 + F[\partial_x \Phi]$, where F is a functional of the spatial derivative of Φ. In the first approximation order there is $F \approx \alpha \partial_x \Phi$. Hence, using this ansatz the equation for R gives $\alpha = -\xi_0^2 p/(\sqrt{g(\epsilon^2 - (\xi_0 p)^2)})$. In addition, the phase perturbation equation can be approximated as $\partial_t \Phi \approx J_0(\partial_{xx}\Phi + 2pR^{-1}\partial_x R)$, where $J_0 = \xi_0^2/\tau_0$. Hence, expanding R^{-1} as $R^{-1} \approx R_0^{-1}$ the Eq. (55) is reduced to

$$\partial_t \Phi = D_1 \partial_{xx}\Phi, \tag{56}$$

where $D_1 = J_0(1 + 2\alpha p/R_0)$. Eq. (56) is a well-known linear diffusion equation.

Fig. 10 shows a three-dimensional representation of Φ and we can observe the typical diffusive behavior. Note that, this equation is not valid for $D_1 = 0$ which occurs at $p_E = \sqrt{3}\epsilon/(3\xi_0)$. When $D_1 < 0$ a nonlinear expansion must be utilized. Consequently, in the next order of the expansion, the functional F is approximated by $F \approx \alpha\partial_x\Phi + \beta\partial_x^3\Phi$. Using the equation for R we find α unchanged while $\beta = -\xi_0^4 p/(\sqrt{g}(\epsilon^2 - (\xi_0^2 p)^2)^{3/2})$. Also, expanding R^{-1} as

$$R^{-1} \approx R_0^{-1}(1 - (\alpha/R_0)\partial_x\Phi - (\beta/R_0)\partial_{xxx}\Phi) + R_0^{-1}(\alpha/R_0)^2(\partial_x\Phi)^2 + \cdots, \tag{57}$$

and taking into account the terms of the fourth order in the spatial derivatives, Eq. (55) can be cast in the form

$$\partial_t \Phi = D_1\partial_{xx}\Phi + D_2\partial_{xxxx}\Phi + D_3\partial_{xx}\Phi\partial_x\Phi - D_4(\partial_x\Phi)^2\partial_{xx}\Phi, \tag{58}$$

where $D_2 = 2J_0\beta p/R_0$, $D_3 = 2J_0\alpha(1 - \alpha p/R_0)/R_0$ and $D_4 = 2J_0\alpha^2(1 - \alpha p/R_0)/R_0^2$. This equation is a Cahn–Hilliard like equation [66]. Depending on the sign of the coefficients D_j, this equation will contain all the dynamical behavior of the phase. However, in many convection cases the type of Eq. (58) has a divergent behavior [67]. This problems can enhance when higher spatial derivatives are taken into account [67,68].

6. Final remarks

In the present work, Rayleigh–Benard convection in a magnetic fluid in a carrier viscoelastic liquid is studied. We determine the stability threshold for the stationary convection for free–free boundary conditions and get the same results already obtained by Finlyson [21]. A weakly nonlinear analysis was performed and the analytical expressions for the coefficients of the corresponding amplitude equation were obtained. We found that the viscoelastic effects appear in the growth rate amplitude and in the nonlinear coefficient. Due to the rheological properties a subcritical–supercritical transition can be obtained. Let us comment that, very often ferrofluids show a finite solutal separation ratio and magnetic separation ratio requiring a binary mixture description; however, for materials where the separation ratio and magnetic separation ratio are not too large, the simple fluid approximation can be used [28]; and the present work is based on this feature.

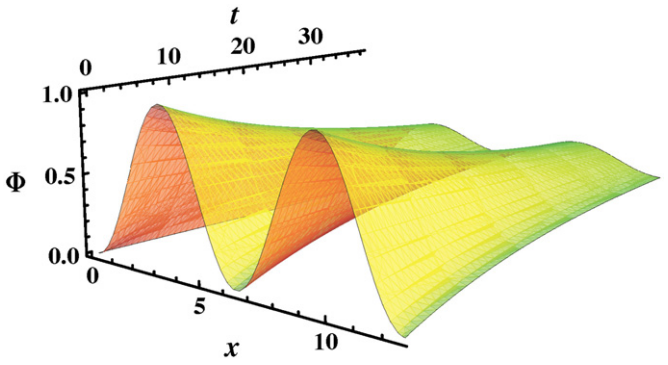


Fig. 10. Φ as a function of space-time for model (54) at $D_1 = 1/20$ and a $\sin^2(x)$ initial condition.

Acknowledgments

We would like to thank Professor H. Pleiner by useful discussions and his critical reading of the manuscript. D.L. acknowledges the financial support from FONDECYT 11080229, Millenium Scientific Initiative, P06-022-F, Financiamiento Basal para Centros Cientificos y Tecnologicos de Excelencia CEDENNA and *Convenio de Desempeño* UTA Mineduc. R.R. acknowledges FONDECYT 11080286 and Postdoctoral program fellowship of Bicentennial Program of Sciences and Technology-Chile. L.M.P acknowledges the USACH Ph.D. program fellowship.

Appendix A

In this manuscript Eq. (19) is $\pounds\mathbf{u} + \mathbf{N}(\mathbf{u}|\mathbf{u}) = 0$, where $\pounds$ is the spatio-temporal linear operator and $\mathbf{N}$ stands for the nonlinear part. These functions can be cast in the form

$$\pounds = \begin{pmatrix} \partial_t\nabla^2 & PRa(1+M_1)\partial_x & -PRaM_1\partial_{zz}^2 & -P\nabla^2 & -P\partial_{xz}^2 & 0 \\ \partial_x & \partial_t - \nabla^2 & 0 & 0 & 0 & 0 \\ 0 & \partial_z & -(\partial_{zz}^2 + M_3\partial_{xx}^2) & 0 & 0 & 0 \\ -(\Gamma\Lambda\partial_t + 1)\nabla^2 & 0 & 0 & 1 + \partial_t\Gamma & 0 & 0 \\ -4(\Gamma\Lambda\partial_t\partial_{xx}^2 + \partial_{xz}^2) & 0 & 0 & 0 & 1 + \partial_t\Gamma & 0 \\ 0 & 0 & 0 & 0 & 0 & 1 + \partial_t\Gamma \end{pmatrix}, \tag{A.1}$$

and

$$\mathbf{N} = \begin{pmatrix} -J(\psi, \nabla^2\psi) + PRaM_1\partial_z\theta\nabla^2\phi \\ -J(\psi,\theta) \\ 0 \\ \Gamma\Lambda[J(\psi,\Lambda^2\psi) + 2(\partial_{xz}^2\psi)\nabla^2\psi] - \Gamma\left[J(\psi,\tau) + \frac{1}{2}(\nabla^2\psi)S - \frac{1}{2}\mathbf{a}(\partial_{xz}^2\psi)U\right] \\ \Gamma\Lambda[4J(\psi,\partial_{xz}^2\psi) - 2(\nabla^2\psi)(\Lambda^2\psi)] + \Gamma[-J(\psi,S) + 2(\nabla^2\psi)\tau + 2\mathbf{a}(\partial_{xz}^2\psi)S] \\ 2\Gamma\Lambda\mathbf{a}[4(\partial_{xz}^2\psi)(\partial_{xz}^2\psi) + (\Lambda^2\psi)(\nabla^2\psi)] - \Gamma[-J(\psi,U) + 2\mathbf{a}(\nabla^2\psi)\tau + 2\mathbf{a}(\partial_{xz}^2\psi)S] \end{pmatrix}, \tag{A.2}$$

where $J(f,g) = \partial_x f\partial_z g - \partial_z f\partial_x g$ and $\Lambda^2 = \partial_{zz}^2 - \partial_{xx}^2$.

References

[1] B.M. Berkovsky, V.F. Medvdev, M.S. Krakov, The Magnetic Fluids, Engineering Application, Oxford University Press, Oxford, 1973.
[2] M. Mahmoudi, et al., J. Phys. Chem. C 113 (2009) 2322.
[3] E.H. Kim, Y. Ahn, H.S. Lee, J. Alloys Compd. 434 (2007) 633.
[4] C. Alexiou, et al., J. Drug Targeting 11 (2003) 139.
[5] C. Alexiou, et al., J. Magn. Magn. Mater. 252 (2002) 363.
[6] C. Alexiou, et al., Cancer Res. 60 (2000) 6641.
[7] A.S. Popel, P.C. Johnson, Ann. Rev. Fluid Mech. 37 (2005) 43.
[8] O.K. Baskurt, H.J. Meiselman, Semin. Thromb. Hemostatis 29 (2003) 435.
[9] J.J. Bishop, Biorheology 38 (2001) 263.
[10] H. Shahnazian, et al., J. Phys. D Appl. Phys. 42 (2009) 205004.
[11] D. Yu Borin, S. Odenbach, J. Phys. Condens. Matter 21 (2009) 246002.
[12] S.A. Lira, J.A. Miranda, Phys. Rev. E 80 (2009) 046313.
[13] S.A. Lira, J.A. Miranda, Phys. Rev. E 79 (2009) 046303.
[14] O. Müller, D. Hahn, M. Liu, J. Phys. Condens. Matter 18 (2006) S2623.
[15] P. Ilg, M. Kröger, S. Hess, Phys. Rev. E 71 (2005) 031205.
[16] S. Odenbach, J. Phys. Condens. Matter 16 (2004) R1135.
[17] S. Odenbach, J. Phys. Condens. Matter 15 (2003) S1497.
[18] H.W. Müller, M. Liu, Phys. Rev. E 64 (2001) 061405.
[19] B.J. de Gans, C. Blom, A.P. Philipse, J. Mellema, Phys. Rev. E 60 (1999) 4518.
[20] J.L. Neuringer, R.E. Rosensweig, Phys. Fluids 7 (1964) 1927.
[21] B.A. Finlayson, J. Fluid Mech. 40 (1970) 753.
[22] K. Gotoh, M. Yamada, J. Phys. Soc. Jpn 51 (1982) 3042.
[23] P.J. Blennerhassett, F. Lin, P.J. Stiles, Proc. R. Soc. London A 433 (1991) 165.
[24] M.D. Gupta, A.S. Gupta, Int. J. Eng. Sci. 17 (1979) 271.
[25] S. Venkatasubramanian, P.N. Kaloni, Int. J. Eng. Sci. 32 (1994) 237.
[26] P.N. Kaloni, J.X. Lou, J. Magn. Magn. Mater. 284 (2004) 54.
[27] G. K Auernhammer, H.R. Brand, Eur. Phys. J. B 16 (2000) 157.
[28] A. Ryskin, H. Pleiner, Phys. Rev. E 69 (2004) 046301.
[29] D. Laroze, J. Martinez-Mardones, J. Bragard, P. Vargas, Physica A 371 (2006) 46.
[30] D. Laroze, J. Martinez-Mardones, L.M. Pérez, Y. Rameshwar, Int. J. Bifurc. Chaos 19 (2009) 2755.
[31] Y. Qin, P.N. Kaloni, Eur. J. Mech. B/Fluids 13 (1994) 305.
[32] I.S. Shivakumara, N. Rudraiah, C.E. Nanjundappa, J. Magn. Magn. Mater. 248 (2002) 379.
[33] P.N. Kaloni, J.X. Lou, Phys. Rev. E 70 (2004) 026313.
[34] P.N. Kaloni, J.X. Lou, Phys. Rev. E 71 (2005) 066311.
[35] Sunil, P. Sharma, A. Mahajan, Heat Transfer Res. 40 (2009) 351.
[36] Sunil, P. Chandb, P.K. Bhartia, A. Mahajan, J. Magn. Magn. Mater. 320 (2008) 316.
[37] S. Odenbach, Th. Volker, J. Magn. Magn. Mater. 289 (2005) 122.
[38] D.D. Joseph, Fluid Dynamics of Viscoelastic Liquids, Springer, New York, 1990.
[39] C.M. Vest, A. Arpaci, J. Fluid Mech. 36 (1969) 613.
[40] M. Sokolov, R.I. Tanner, Phys. Fluids 15 (1972) 534.
[41] R.W. Kolkka, G.R. Ierly, J. Non-Newtonian Fluid Mech. 25 (1987) 299.
[42] J. Martinez-Mardones, C. Perez-Garcia, J. Phys. Condens. Matter 2 (1990) 1981.
[43] J. Martinez-Mardones, R. Tiemann, W. Zeller, C. Perez-Garcia, Int. J. Bifurc. Chaos 4 (1994) 1347.
[44] J. Martinez-Mardones, R. Tiemann, W. Zeller, Chaos, Solitons Fractals 6 (1995) 341.
[45] J. Martinez-Mardones, R. Tiemann, D. Walgraef, W. Zeller, Phys. Rev. E 54 (1996) 1478.
[46] H.M. Park, H.S. Lee, J. Non-Newtonian Fluid Mech. 60 (1995) 1.
[47] H.M. Park, H.S. Lee, J. Non-Newtonian Fluid Mech. 66 (1996) 1.
[48] P. Kolodner, J. Non-Newtonian Fluid Mech. 75 (1998) 167.
[49] J. Martinez-Mardones, R. Tiemann, D. Walgraef, J. Non-Newtonian Fluid Mech. 93 (2000) 1.
[50] J. Martinez-Mardones, R. Tiemann, D. Walgraef, Physica A 327 (2003) 29.
[51] D. Laroze, J. Martinez-Mardones, C. Perez-Garcia, Int. J. Bifurc. Chaos 15 (2005) 3329.
[52] D. Laroze, J. Martinez-Mardones, J. Bragard, C. Perez-Garcia, Physica A 385 (2007) 433.
[53] D. Laroze, J. Martinez-Mardones, J. Bragard, Eur. Phys. J. Spec. Top. 146 (2007) 291.
[54] D. Laroze, J. Martinez-Mardones, AIP Conf. Proc. 913 (2007) 9.
[55] D. Laroze, J. Martinez-Mardones, L.M. Pérez, Int. J. Bifurc. Chaos 20 (2010) 235.
[56] H. Pleiner, M. Liu, H.R. Brand, Rheol. Acta 43 (2004) 502.
[57] T.T. Perkins, D.E. Smith, S. Chu, Science 276 (1997) 2016.
[58] S.R. Quake, H. Babcock, S. Chu, Nature 388 (1997) 151.
[59] H. Babcock, D.E. Smith, J.S. Hur, E.S.G. Shaqfeh, S. Chu, Phys. Rev. Lett. 85 (2000) 2018.
[60] A.C. Newell, J.A. Whitehead, J. Fluid Mech. 38 (1969) 279.
[61] L.A. Segel, J. Fluid Mech. 38 (1969) 203.
[62] M.C. Cross, P.C. Hohenberg, Rev. Mod. Phys. 65 (1993) 851.
[63] L. Kramer, W. Zimmermann, Physica D 16 (1985) 221.
[64] L. Tuckerman, D. Barkley, Physica D 46 (1990) 57.
[65] M. Argentina, O. Descalzi, E. Tirapegui, Int. J. Bifurc. Chaos 11 (2002) 2459.
[66] J.W. Cahn, J.E. Hilliard, J. Chem. Phys. 28 (1958) 258.
[67] H. Riecke, Europhys. Lett. 11 (1990) 213.
[68] H. Riecke, Physica D 82 (1995) 79.